Mechanisms of the Reactions of W and W^+ with H_2O: Computational Studies

D. G. Musaev,* S. Xu, S. Irle,* and M. C. Lin*

Cherry L. Emerson Center for Scientific Computation and Department of Chemistry, Emory University, 1515 Dickey Drive, Atlanta, Georgia 30322

Received: August 19, 2005; In Final Form: February 13, 2006

The mechanism of the reactions of W and W^+ with the water molecule have been studied for several lower-lying electronic states of tungsten centers at the CCSD(T)/6-311G(d,p)+SDD and B3LYP/6-31G(d,p)+SDD levels of theory. It is shown that these reactions are essentially multistate processes, during which lower-lying electronic states of the systems cross several times. They start with the formation of initial prereaction $M(H_2O)$ complexes with $M-H_2O$ bonding energies of 9.6 and 48.2 kcal/mol for M = W and W^+, followed by insertion of the metal center into an O−H bond with 20.0 and 53.3 kcal/mol barriers for neutral and cationic systems, respectively. The overall process of $M + H_2O \rightarrow$ *t*-HM(OH) is calculated to be highly exothermic, 48.4 and 48.8 kcal/mol for M = W and W^+. From the HM(OH) intermediate the reaction may proceed via several different channels, among which the stepwise $HM(OH) \rightarrow HMO + H \rightarrow (H)_2MO$ and concerted $HM(OH) \rightarrow (H)_2MO$ pathways are more favorable and can compete (energetically) with each other. For the neutral system (M = W), the concerted process is the most favorable, whereas for the charged system ($M = W^+$), the stepwise pathway is slightly more favorable. From the energetically most favorable intermediate $(H)_2MO$ the reactions proceed via H_2-molecule formation with a 53.1 kcal/mol activation barrier for the neutral system. For the cationic system, H−H formation and dissociation is an almost barrierless process. The overall reaction of W and W^+ with the water molecule leading to $H_2 + MO$ formation is found to be exothermic by 48.2 and 39.8 kcal/mol, respectively. In the gas phase with the collision-less conditions the reactions $W(^7S) + H_2O \rightarrow H_2 + WO(^3\Sigma^+)$, and $W^+(^6D) + H_2O \rightarrow H_2 + WO^+(^4\Sigma^+)$ are expected to proceed via a 10.4 and 5.1 kcal/mol overall energy barrier corresponding to the first O−H dissociation at the TS1. On the basis of these PESs, we predict kinetic rate constants for the reactions of W and W^+ with H_2O.

Introduction

Understanding the mechanisms and the factors governing the reactions of transition-metal systems with small molecules (such as N_2, CO, CO_2, O_2, H_2O, etc.) is an essential prerequisite for designing novel and more effective catalysts, for instance for nitrogen fixation, hydrocarbon hydroxylation, utilization of carbon mono- and di-oxides, as well as for the preparation of new materials with advanced physicochemical properties. The knowledge of numerous factors such as redox activities and spin states of transition-metal centers, the nature of their ligand environment, the identity of reactive intermediates, the nature of substrate, solvent and support materials are all crucial for designing better catalysts and better materials. The first step toward elucidating these various aspects is to study the gas-phase reactions of transition-metal (TM) atoms and ions, which are free from ligand, solvent, and support effects. Such studies are particularly useful to provide information concerning the dependence of the reactivity of TM species on the electronic and spin states of the TM atoms and ions in these reactions. To obtain atomistic level understanding of these reactions with the experiments,[1] state-of-the-art calculations of their potential energy surfaces (PESs) owing to several low-lying electronic states of reactants, intermediates and products of the gas-phase reaction become vital and are expected to give information essential not only for interpretation of experimental results but also for a comprehensive understanding of more complicated reactions involving TM systems.

In this paper we study the reaction of W and W^+ with the water molecule. Tungsten and tungsten alloys are widely used in high-temperature environments where arc ablation or mechanical deformation and damage are the main sources of materials failure.[2] Hence, the thermal reaction of tungsten with gas molecules or radicals has brought about strong interests to scientists. Hamamura performed a series of experimental studies for the thermal reaction between water vapor and a tungsten filament at extremely low pressures in the temperature range $T = 1270-2460$ K.[3] The authors obtained W oxide deposit of $WO_{2.8}$ when *T* was below 1950 K and showed that the O/W ratio of the deposit increases from $WO_{2.83}$ to $WO_{3.93}$ upon an increase of temperature from 2000 to 2460 K. Hamamura also studied the effect of the partial pressure of H_2 in these reactions,[4] and the reactions of other gases such as NO, N_2, O_2 on the surface of tungsten.[5] Many other experiments on the reaction mechanism of water on W surfaces were also reported.[6] It was shown that the adsorption of water on the W surface had dissociative character $H_2O \rightarrow OH + H$, and that desorption proceeds via a surface reaction $OH + OH \rightarrow H_2O + O$. The free O subsequently oxidizes W to WO_3.

Previously, many high-level computational methods were applied to elucidate the reaction mechanisms of transition-metal atoms and cations with several small molecules.[7] Water is one of the most important molecular species; however, to our knowledge, there has been no theoretical investigation of the reaction mechanisms of water with W and W^+. In this work, we detail our study of the mechanisms and reaction rates of the

10.1021/jp054683m CCC: $33.50
Published on Web 03/09/2006

TABLE 1: Comparison the Calculated and Experimental Values of the Excitation (of W and W^+) and Ionization (of W and WO) Energies, as well as Heat of the Reactions $W(^7S) + H_2O \rightarrow WO + H_2$, $W(^7S) + H_2O \rightarrow WH + OH$, $W^+(^6D) + H_2O \rightarrow WO^+ + H_2$, and $W^+(^6D) + H_2O \rightarrow WH^+ + OH$ (All Values in kcal/mol)

excitation and ionization energies			heats of the reaction		
process	calcd	exp	reaction[a]	calcd	exp[e]
$W\ (^7S \rightarrow {}^5D)$	4.6	4.3[a]	$W\ (^7S)/W^+(^6D) + H_2O$	0.0	
$W\ (^7S \rightarrow {}^3P)$	45.0	37.9[b]	$WO(^3\Sigma^+) + H_2$	−48.2	-56 ± 17
$W\ (^7S \rightarrow {}^1S)$	71.5		$WO(^1\Sigma^+) + H_2$	−25.8	
$W^+\ (^6D \rightarrow {}^4F)$	27.6		$WH(^5\Sigma^+) + OH$	51.3	
$W^+\ (^6D \rightarrow {}^2P)$	47.0	43.6[b]	$WO^+(^2\Sigma^+) + H_2$	−16.9	
IE $[W(^7S) \rightarrow W^+(^6D)]$	171.0	181.3438 ± 0.002[c]	$WO^+(^4\Sigma^+) + H_2$	−39.8	-52.0 ± 23.9
IE $[WO(^3\Sigma^+) \rightarrow WO^+(^4S^+)]$	179.4	186.8 ± 6.9[d]	$WH^+(^5\Sigma^+) + OH$	59.0	66.5 ± 1.3

[a] See ref 21. [b] See ref 20. [c] See ref 16. [d] See ref 17. [e] Experimental heats of the reactions at 0 K were calculated based-on $\Delta_f H_0(H_2O) = -57.10$ kcal/mol (ref 15); $\Delta_f H_0(W) = 203.401$ kcal/mol deduced by $\Delta_f H_{298}(W) = 203.401$ kcal/mol (ref 15); $\Delta_f H_0(W^+) = 384.449$ kcal/mol deduced by equation of $\Delta_f H_{298}(W^+) = \Delta_f H_{298}(W) + IE(W)$, where $IE(W) = 181.3438 \pm 0.002$ kcal/mol (ref 160; $\Delta_f H_0(WO) = 90.136 \pm 17$ kcal/mol deduced by $\Delta_f H_{298}(WO) = 90.136 \pm 17$ kcal/mol (ref 17); $\Delta_f H_0(WO^+) = 375.767 \pm 23.9$ kcal/mol deduced by equation of $\Delta_f H_{298}(WO^+) = \Delta_f H_{298}(WO) + IE(WO)$, where $IE(WO) = 185.633 \pm 6.9$ kcal/mol (ref 17; $\Delta_f H_0(WH^+) = 384.627 \pm 1.2$ kcal/mol deduced by equation of $\Delta_f H_{298}(WH^+) = \Delta_f H_{298}(W^+) + \Delta_f H_{298}(H) - D_0(W^+{-}H)$, where $\Delta_f H_{298}(H) = 52.1$ kcal/mol (ref 15), and $D_0(W^+{-}H) = 52.34 \pm 1.2$ kcal/mol (ref 18); $\Delta_f H_0(H_2) = 0.0$ kcal/mol (ref 15); and $\Delta_f H_0(OH) = 8.85 \pm 0.07$ kcal/mol.

$H_2O + W/W^+$ reaction with several low-lying electronic states of W and W^+.

Computational Procedures

All calculations were performed using the Gaussian 03 suite of programs.[8] The geometries of reactants, intermediates, transition states and products were optimized without imposing symmetry constraints using the B3LYP density functional approach, which combines Becke's generalized gradient correction, Lee−Yang−Parr's nonlocal correlation functional, and exact Hartree−Fock exchange.[9] This functional has been demonstrated to give results superior to those obtained by using pure density functional theory without Hartree−Fock exchange due to a more accurate description of the density of states near the Fermi energy, which is particularly important for TM chemistry.[10] It is worth pointing out that quite surprisingly, the B3LYP hybrid functional is able to predict the thermochemistry of molecules containing transition-metal elements well although no transition-metal compounds were included in the fit.[11] For the B3LYP geometry optimizations we use the Stuttgart/Dresden relativistic effective core potential (ECP)[12] and associated triple-ζ SDD basis set for W, and the 6-31G(d,p) basis set for main group elements. The nature of all stationary points was confirmed by performing a normal-mode analysis. In addition, the nature of the calculated transition states was clarified using the intrinsic reaction coordinate (IRC) approach.[13] The energetics of the optimized structures were improved by performing single point CCSD(T) calculations using the slightly larger basis set 6-311G(d,p) for main group elements and the SDD effective core potential and basis set for W. Unscaled zero-point energy corrections estimated at the B3LYP level were added to the final CCSD(T) energetics. The single determinant nature of the wave function of all stationary points was confirmed by performing T1 diagnostics (T1 parameter for all structures is calculated to be within 0.01−0.06). We also have checked $\langle S^2 \rangle$ values to evaluate the spin contamination in these calculations. As seen from the materials (Table S3) given in the Supporting Information, in general, spin contamination in these calculations is not significant, and maximum contamination from the highest spin states is less than 7%.

As can be seen below, PESs of the several lower-lying electronic states of the studied reactions cross several times upon completion of the reactions. A search for the exact minima on the seam of crossing of these PESs would require the use of computationally much more demanding methods that include the effect of spin−orbit-coupling (SOC) in the calculations. Because of technical limitations, in this paper, we did not perform SOC calculations and did not search for the minima on the seam of crossing of PESs of the studied reactions.

Throughout the paper we discuss the CCSD(T) energetics, and the B3LYP energetics are included in the Supporting Information (both the total and relative energies). We also have included the CCSD(T) total energies and the Cartesian coordinates of all B3LYP optimized structures in the Supporting Information.

The rate constants for the $W + H_2O$ and $W^+ + H_2O$ reactions were calculated using the variational RRKM theory as implemented in the Variflex code.[14]

In Table 1, we compare the available experimental data[15−20] on the excitation and ionization energies, as well as the heats of the reactions $W(^7S) + H_2O \rightarrow WO + H_2$, $W(^7S) + H_2O \rightarrow WH + OH$, $W^+(^6D) + H_2O \rightarrow WO^+ + H_2$, and $W^+(^6D) + H_2O \rightarrow WH^+ + OH$ with their calculated values. As seen from this table the standard deviation between the calculated and experimental data is only ±13.3%, whereas in many cases (especially for excitation and ionization energies) the calculated and experimental data are very close to each other. One should also note that the errors for the reported heats of the reactions $W(^7S) + H_2O \rightarrow WO(^3\Sigma^+) + H_2$, $W^+(^6D) + H_2O \rightarrow WO^+(^4\Sigma^+) + H_2$ are very large. Below, we will discuss these findings in more detail.

Results and Discussions

1. Potential Energy Surfaces of the Reactions of W and W^+ with Water. CCSD(T) predicts the ground electronic spin state of the W atom to be a septet ^7S state associated with the s^1d^5 electronic configuration, whereas the quintet ^5D state associated with the s^2d^4 electronic configuration is slightly, 4.6 kcal/mol, higher in energy. The calculated energy gap between the ^7S and ^5D states, 4.6 kcal/mol, of the W atom very well agrees with its reported experimental value of 4.3 kcal/mol.[21] The CCSD(T) also predicts that the triplet ^3P (s^2d^4) and singlet ^1S (s^2d^4) states of W lie 45.0 and 71.5 kcal/mol higher in energy, respectively. Meanwhile, the ground electronic state of W^+ is the sextet ^6D state associated with the s^1d^4 electronic configuration: its quartet ^4F (s^1d^4) and doublet ^2P (s^1d^4) states are 27.6 and 47.0 kcal/mol higher in energies, which are in good agreement with 24.9 and 43.6 kcal/mol experimental values, respectively.[20] The ionization energy of the W atom is calculated to be 171.0 kcal/mol, which is in excellent agreement with the

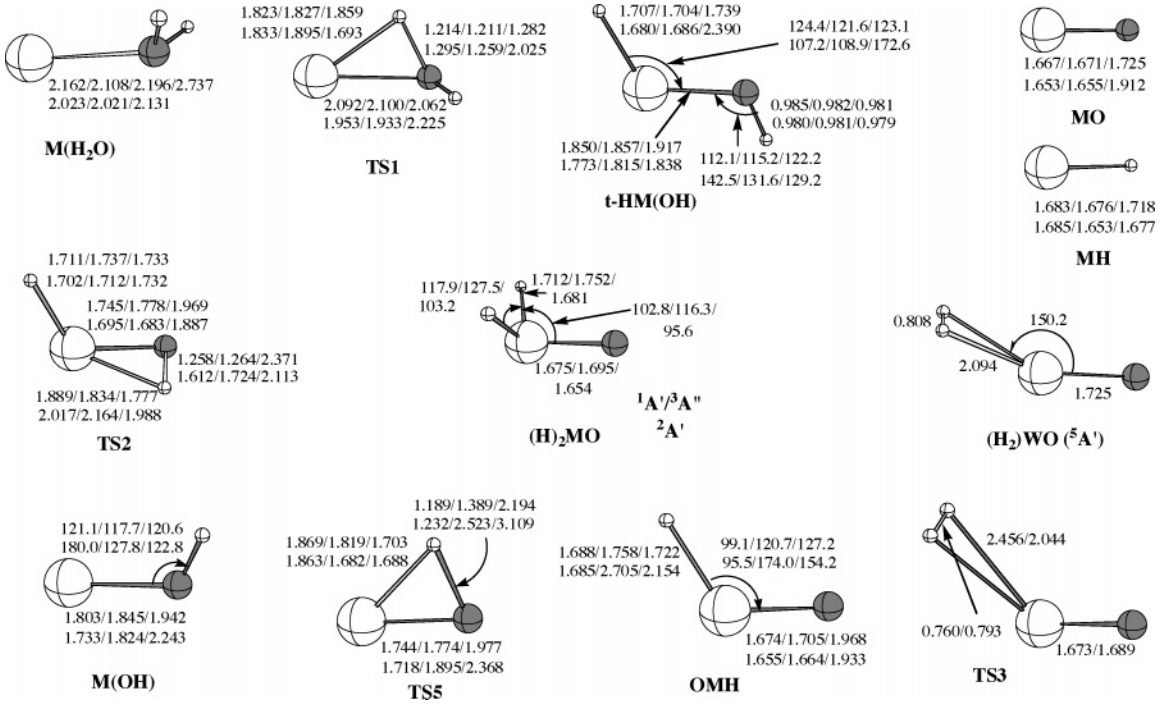

Figure 1. Calculated important geometry parameters (distances in Å and angles in deg) of the intermediates, transition states and products of the reactions W + H_2O (the first line) and W^+ + H_2O (the second line) occurring on various low-lying electronic states: for **M(H_2O)**, **TS1**, ***t*-HM-(OH)**, **TS2**, **TS3**, and **$(H)_2$MO** at their singlet/triplet/quintet (and septet for **W(H_2O)**) and sextet/quartet/doublet states for M = W and W+, respectively; for **MH**, **M(OH)**, **TS5** and **HMO** at their sextet/quartet/doublet and singlet/triplet/quintet/septet states for M = W and W^+, respectively.

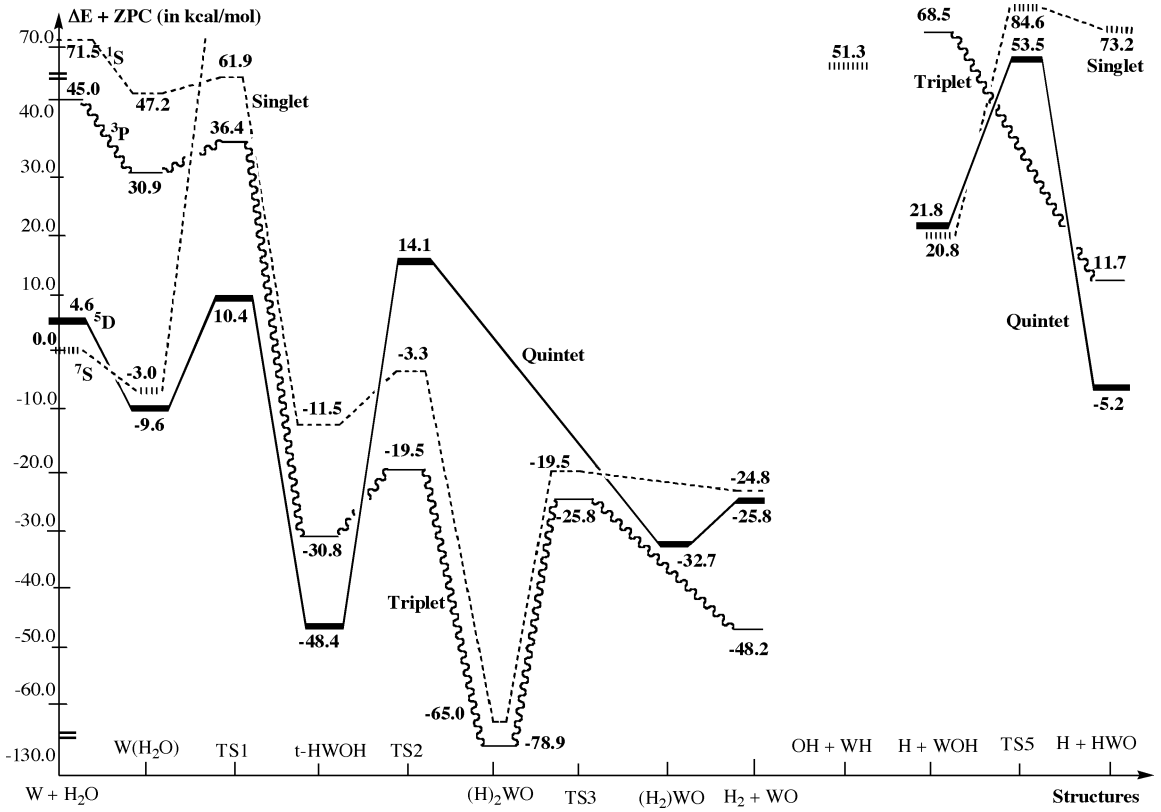

Figure 2. Schematic presentation of the PES of the reaction W + H_2O on various low-lying electronic states showing reactants, intermediates and products.

experimental value of 181.3438 ± 0.002 kcal/mol.[16] Below we present potential energy surfaces (PESs) for the reaction of water with the W atom in its ^7S, ^5D, ^3P and ^1S spin states, whereas the reaction of W^+ + H_2O is investigated under the consideration of the ^6D, ^4F, and ^2P states of the tungsten cation. The calculated structures of all intermediates, transition states and products of all investigated reactions are given in Figure 1. Figures 2 and 3 include the calculated PESs of the reaction of M = W and W^+ with water, respectively.

As one might expect, the first step of the reaction is the coordination of the water molecule to the M-center to form a prereaction aqua complex, M(H_2O). As shown in Figure 2, for

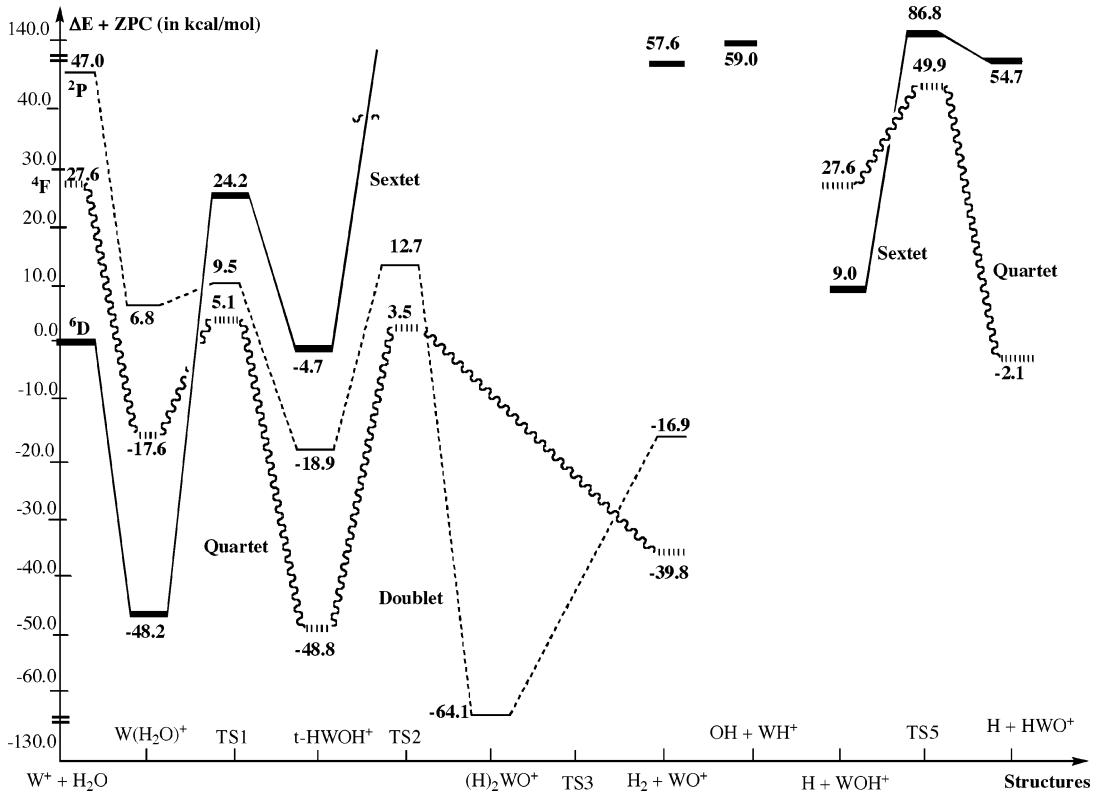

Figure 3. Schematic presentation of the PES of the reaction $W^+ + H_2O$ on various low-lying electronic states showing reactants, intermediates and products.

the W atom, the formation of the initial $W(H_2O)$ complex occurs via a septet to quintet spin-flip, resulting in the quintet $^5A'$ ground state of the aqua-complex. Its $^7A'$, $^3A''$ and $^1A'$ states are 6.6, 40.5 and 56.8 kcal/mol higher in energy relative to the $^5A'$ ground state, respectively. These findings can be explained by the fact that the low spin states of W have empty orbitals, which can effectively bind OH_2, whereas in its high ^7S spin state all orbitals are occupied and consequently, the water molecule is weakly bound. Figure 3 shows that for W^+ there is no spin-flip at the beginning of the reaction and the coordination of water leads therefore to a sextet $^6A'$ ground-state $W(H_2O)^+$ complex with its $^4A'$ and $^2A'$ states being 30.6 and 55.0 kcal/mol higher in energy. The lack of spin-flip at the beginning of the reaction is result of existence empty orbitals in all lower-lying electronic states of W^+, which can equally strongly bind water molecule. The calculated (ground state to ground state) $W-H_2O$ and W^+-H_2O bonding energies are 9.6 and 48.2 kcal/mol, respectively. Unfortunately, no experimental data are available for comparison.

At the next stage of the reaction, insertion of the metal center into the O−H bond occurs, which leads to the formation of HM(OH) products. The transition states (TS1) associated with these processes are characterized by significant O−H bond weakening going from 0.98 Å in prereaction complexes to 1.2−1.3 Å at the TSs, except for the sextet $^6A'$ state of $W(H_2O)^+$, where the O−H bond is already essentially broken with r(O−H) = 2.025 Å. The calculated barriers of the neutral system (from the corresponding prereaction aqua-complex) are 20.0, 5.5 and 14.7 kcal/mol for quintet, triplet and singlet states, respectively. On the septet-state surface, the O−H bond activation is energetically very high and will not be discussed. For the cationic system, the calculated barriers are 72.4, 22.7 and 3.7 kcal/mol for sextet, quartet and doublet states, respectively. Noticeable is the high barrier of 72.4 kcal/mol for the O−H bond activation by W^+ calculated from the sextet ground state of the $W(H_2O)^+$ complex, which is larger by about 50 kcal/mol than the corresponding barrier from the quintet ground state of the neutral $W(H_2O)$ complex, indicating the high energy of the $HWOH^+$ high spin state. However, as can be seen in Figure 3, for the cationic system, the O−H bond cleavage occurs energetically more favorably via a sextet to quartet spin-crossing: the reaction starts from the sextet $^6A'$ ground state of $W(H_2O)^+$ but proceeds via the quartet transition state. As a result, the barrier for the O−H cleavage calculated from the ground $^6A'$ state of prereaction complex $W(H_2O)^+$ to the ground $^4A'$ state of TS1 is reduced to 53.3 kcal/mol, which is still larger than that for the neutral system (20.0 kcal/mol). The major reason of the large O−H bond activation barrier by W^+ compared to that for W neutral system is the strong stabilization of W^+-H_2O bond (48.2 kcal/mol) compared to $W-H_2O$ (9.6 kcal/mol), which is mainly due to the existence of the positive charge in the former.

The product of the O−H bond activation is the hydrido−metal−hydroxy complexes, HM(OH), which can exist as cis and trans isomers with the hydrogens in cis and trans to each other, respectively. Though we have calculated both isomers, as well as the transition state (TS4) separating these isomers, below we discuss only the energetically slightly more favorable trans isomer. We included the energies and geometries of cis isomers and TS4s in the tables of the Supporting Information. The ground electronic state of the neutral *t*-HW(OH) intermediate is the quintet ^5A state, with triplet ^3A and singlet ^1A states being 17.6 and 36.9 kcal/mol higher in energy, respectively. The overall process of $W(^7S) + H_2O \rightarrow$ *t*-HW(OH) (^5A) is calculated to be exothermic by 48.4 kcal/mol.

The ground electronic state of the cationic *t*-$HW(OH)^+$ intermediate of the reaction $W^+ + H_2O$ is the quartet ^4A state, with doublet and sextet states being 29.9 and 44.1 kcal/mol higher in energy, respectively. The exothermicity of the reaction

$W^+(^6D) + H_2O \rightarrow t\text{-}HW(OH)^+$ (^4A), 48.8 kcal/mol, is almost the same as that of the neutral process $W(^7S) + H_2O \rightarrow t\text{-}HW(OH)$ (^5A).

From the hydrido−metal−hydroxy intermediate HM(OH), the reaction may proceed via several different channels: (a) the separation of the OH ligand leading to the formation of OH + MH products, (b) the dissociation of the H ligand leading to the formation of H + M(OH), followed by activation of the O−H bond to form the HMO product, (c) the breaking of the O−H bond to form HMO, and (d) the activation of the second O−H bond to form the dihydrido−metal−oxide $(H)_2MO$ species by an isomerization reaction.

The dissociation of the OH ligand is calculated to be highly endothermic for both the neutral and positively charged systems, and therefore unlikely to represent a major channel of the reaction under mild conditions. The dissociation of the H radical leading to the formation of H + M(OH) is calculated to be less endothermic than the OH dissociation channel; however, it is still unlikely to compete with channel (c) starting with cleavage of O−H bond and leading to HMO + H products. The dissociation of O−H bond in HM(OH), pathway (c), is calculated to be 43.2 and 46.7 kcal/mol for neutral and charged systems, respectively. This dissociative (or stepwise) pathway $HM(OH) \rightarrow HMO + H \rightarrow (H)_2MO$ may compete (energetically) with the concerted process (d) starting with activation of the second O−H bond in HM(OH) and leading to the $(H)_2MO$ species. For the neutral system (M = W), the reaction *t*-HW(OH) → $(H)_2WO$ proceeds via a quintet-triplet surface crossing *before* the O−H bond activation transition state TS2 (see Figure 2): the reaction starts from the quintet ground state of *t*-HW(OH), proceeds via a triplet transition state TS2, and finally leads to the triplet $(H)_2WO$ ($^3A'$) product with a relative energy (relative to the reactants) of −78.9 kcal/mol. The barrier (calculated from the quintet ground state to triplet TS2) associated with this process is found to be 28.9 kcal/mol. For the positively charged system ($M = W^+$), the reaction *t*-$HW(OH)^+$ → $(H)_2WO^+$ proceeds likewise via quartet-doublet surface-crossing that occurs *after* the O−H bond activation transition state TS2 (see Figure 3). In other words, the reaction starts from the quartet ground state of *t*-$HW(OH)^+$, proceeds via quartet transition state TS2 and leads to the doublet H_2WO^+ product with a relative energy (relative to the reactants) of −64.1 kcal/mol. The energy barrier associated with this reaction is 52.3 kcal/mol, which again is significantly larger than that for the neutral reaction. The ground-state to ground-state process *t*-HM(OH) → $(H)_2MO$ is calculated to be exothermic by 30.5 and 15.3 kcal/mol for neutral and positively charged systems.

In summary, among the processes starting from the HM(OH) and leading to the energetically most favorable intermediate $(H)_2MO$ the stepwise $HM(OH) \rightarrow HMO + H \rightarrow (H)_2MO$ and concerted $HM(OH) \rightarrow (H)_2MO$ pathways are more favorable and can compete with each other. For the neutral system (M = W), the concerted process that occurs with 28.9 kcal/mol barrier is the most favorable one (calculated barrier on the stepwise pathway is 43.2 kcal/mol). In contrast, for the charged system ($M = W^+$), the stepwise pathway is slightly more favorable: the calculated barriers are 46.7 and 52.3 kcal/mol for stepwise and concerted pathways, respectively.

As can be seen from Figure 1, the complex $(H)_2WO$ has a dihydride structure at its lowest triplet $^3A''$ and singlet $^1A'$ states. However, at the quintet $^5A'$ surface we were not able locate a dihydride structure: all our attempts to locate such a structure lead to dihydrogen $(H_2)WO$ intermediate with H−H bond distance of 0.808 Å, which lies 46.2 kcal/mol higher than lowest triplet state. IRC calculations also confirm that TS2 at the quintet $^5A'$ surface connects *t*-HWOH minimum with the dihydrogen complex $(H_2)WO$. Similarly, for the positively charged systems IRC calculations from the TS2 lead to a dihydride $(H)_2WO^+$ intermediate (with a long H−H bond) in its ground doublet $^2A'$, whereas at the excited quartet $^4A'$ surface TS2 connects *t*-$HWOH^+$ with $H_2 + WO^+(^4A')$ dissociation limit. In the other words, dihydride $(H)_2WO^+$ intermediate does not exists at the $^4A'$ surface. This, as well as absence of $(H)_2WO$ ($^5A'$), can be explain by lack of enough electrons to form these structures with 4 (or 5) W−ligand bonds at their high spin electronic states. Close examination of the PES of reaction for cationic system (Figure 3) shows that *t*-$HWOH^+$ to $(H)_2WO^+$ starts with quartet *t*-$HWOH^+$ reactant, proceeds via 45.3 kcal/mol barrier at the quartet TS2, and crosses doublet surface that leads to doublet dihydride $(H)_2WO^+$ intermediate.

Results presented in Figures 2 and 3 show that the $(H)_2MO$ species is lowest in energy for the $[MH_2O]$ reaction systems, which partially can be explained by the large exothermicity of the tungsten−oxygen bond formation.

From the $(H)_2MO$ intermediates the reactions may proceed via either O-atom dissociation or H_2-molecule formation and elimination or H-atom dissociation to form HMO + H. O-atom elimination is expected to be highly endothermic and was not studied in detail. Although the H-atom dissociation is more favorable than O-atom dissociation, it still cannot effectively compete with the H_2 elimination channel. Calculations show that the hydrogen molecule elimination proceed via H−H bond formation at the TS3 and leads to H_2 + MO products without formation any dihydrogen $(H_2)WO$ intermediate at the singlet and triplet surfaces. The calculated the H−H bond formation barrier is 53.1 and 45.5 kcal/mol for ground triplet and excited singlet states of the neutral system.

For the cationic system, H_2 formation and elimination starts from the doublet $(H)_2WO^+$ intermediate, crosses quartet surface, and leads to quartet products of $H_2 + WO^+(^4A')$. This may occur with a small energy barrier corresponding to doublet to quartet spin-flip, which is not calculated in this paper. We have performed extensive search for the dihydrogen $(H_2)MO$ intermediates, and for possible transition state corresponding to the dihydride $(H_2)MO$ to dihydrogen $(H_2)MO$ rearrangement. Unfortunately, we could not locate the stable dihydrogen $(H_2)MO$ intermediates, except that for quintet state of the neutral system. Despite that, we still could expect the existence of weakly bound (H_2)−MO complex, the existence of which will not affect the calculated mechanisms of the studied reactions.

It is worth noting that the calculated ground-state to ground-state endothermicity of the $(H_2)MO \rightarrow H_2 + MO$ process is 30.7 and 24.3 kcal/mol for M = W and W^+, respectively. These values are significantly lower than those calculated for the formation of H + M(OH) and OH + MH, indicating that the major channel of the reactions of W/W^+ with water molecules is the H_2 + MO formation. As can be seen from Figures 2 and 3, the entire reactions of W and W^+ with a water molecule leading to H_2 + MO formation are exothermic by 48.2 and 39.8 kcal/mol, respectively. As could be expected from these PES's, in the gas phase with the collision-less conditions the reactions $W(^7S) + H_2O \rightarrow H_2 + WO(^3\Sigma^+)$, and $W^+(^6D) + H_2O \rightarrow H_2 + WO^+(^4\Sigma^+)$ will proceed via a 10.4 and 5.1 kcal/mol overall energy barrier corresponding to the first O−H dissociation at the TS1.

One should note that despite the energetic infeasibility of the formation of the M(OH) product, we also have elucidated the

mechanism of the M(OH) → HMO isomerization process (see Figures 1−3). As shown in Figures 2 and 3, the isomerization is exothermic by 26.0 and 11.1 kcal/mol and proceeds via 31.7 and 40.9 kcal/mol barriers of the transition states TS5 for M = W and W^+, respectively.

2. Rate Constant Calculations. On the basis of the aforementioned PESs for the reaction of W/W^+ with the H_2O molecule, we have computed the rate constants for the following seven reactions:

$$W(^1S) + H_2O \rightarrow WO(^1\Sigma^+) + H_2 \quad (1)$$

$$W(^3P) + H_2O \rightarrow WO(^3\Sigma^+) + H_2 \quad (2)$$

$$W(^5D) + H_2O \rightarrow (H)_2WO(^3A'') \rightarrow WO(^3\Sigma^+) + H_2 \quad (3)$$

$$W(^7S) + H_2O \rightarrow W(H_2O)(^5A') \rightarrow (H)_2WO(^3A'') \rightarrow WO(^3\Sigma) + H_2 \quad (4)$$

$$W^+(^2P) + H_2O \rightarrow WO^+(^4\Sigma^+) + H_2 \quad (5)$$

$$W^+(^4F) + H_2O \rightarrow (H)_2WO^+(^2A') \rightarrow WO^+(^4\Sigma^+) + H_2 \quad (6)$$

$$W^+(^6D) + H_2O \rightarrow t\text{-}HW(OH)^+(^4A) \rightarrow (H)_2WO^+(^2A') \rightarrow WO^+(^4\Sigma^+) + H_2 \quad (7)$$

Here, the explicit inclusion of intermediates in reactions (3), (4), (6) and (7) indicates that spin-flips occur at the respective reaction steps.

For the reaction rate constant calculations, the minimum energy paths (MEP) representing the barrierless association processes W + H_2O → W(H_2O) and W^+ + H_2O → W^+(H_2O) were calculated along the reaction coordinate M−O, which is stretched from its equilibrium value to 6 Å with the step size of 0.2 Å. At each fixed M−O distance, the geometry of the M−OH_2 is fully optimized at the B3LYP level. The obtained MEP is approximated with a Morse potential, $V(r) = D_e\{1 - \exp[-\beta(R - R_0)]\}^2$, where R is the reaction coordinate, R_0 is the equilibrium M−O bond distance, and D_e is the bond energy without zero-point energy corrections. The parameters used to find the Morse potential by fitting the MEP are $R_0 = 2.162$, $\beta = 3.02$ Å^{-2}, and $D_e = 25.6$ kcal/mol for W(^{1}S) + H_2O for reaction 1; $R_0 = 2.108$, $\beta = 2.08$ Å^{-2}, and $D_e = 15.0$ kcal/mol for W(^{3}P) + H_2O for reaction 2; $R_0 = 2.196$, $\beta = 2.28$ Å^{-2}, and $D_e = 15.4$ kcal/mol for W(^{5}D) + H_2O for reaction 3; $R_0 = 2.196$, $\beta = 2.28$ Å^{-2}, and $D_e = 10.9$ kcal/mol for W(^{7}S) + H_2O for reaction 4; $R_0 = 2.023$, $\beta = 1.53$ Å^{-2}, and $D_e = 42.2$ kcal/mol for W^+(^{2}P) + H_2O for reaction 5; $R_0 = 2.021$, $\beta = 1.63$ Å^{-2}, and $D_e = 46.8$ kcal/mol for W^+(^{4}F) + H_2O for reaction 6; $R_0 = 2.131$, $\beta = 1.65$ Å^{-2}, and $D_e = 49.8$ kcal/mol for W^+(^{6}D) + H_2O for reaction 7, respectively. Here, β of reaction 4 is assumed to be the same as that of reaction 3 because its MEP crosses that of reaction 3 and they both lead to the same prereaction complex W(H_2O)(^{5}A′).

In view of the fact that the gas-phase reactions of W and W^+, particularly their excited states, which can in principle be produced by laser ablation under low-pressure conditions, our calculations have been carried out under the low-pressure, second-order condition (for example, at 1×10^{-7} Torr molecular beam pressure). In our calculations the effects of multiple reflections above the complex wells were neglected.[22] Similarly, because of the heavy mass and the deep wells of the present system we assume the probability for surface crossing to be unity. All calculations were carried out with the Variflex code, which also includes the reverse reaction into consideration: If the exit barrier forming products is higher than the entrance barrier, the reverse reaction becomes significant as in reaction 4 giving rise to small rate constant.

Under the low-pressure condition, the predicted branching ratios for final product of formation for all but reaction 4 were found to be unity in the broad temperature range 200−3000 K; their second-order rate constants (in molecular units, cm^3/s) can be represented by

$$k_1 = 4.3 \times 10^{-10} T^{0.06} \exp[28/T]$$

$$k_2 = 4.8 \times 10^{-9} T^{-0.31} \exp[-33/T]$$

$$k_3 = 5.4 \times 10^{-16} T^{1.58} \exp[-2443/T]$$

$$k_5 = 1.4 \times 10^{-8} T^{-0.32} \exp[-1648/T]$$

$$k_6 = 3.1 \times 10^{-8} T^{-0.31} \exp[-65/T]$$

$$k_7 = 7.2 \times 10^{-17} T^{1.77} \exp[-2004T]$$

Reaction 4, which has a high barrier (10.4 kcal/mol), was predicted to give H_2 + WO products with negligibly small yields below 500 K and approaching 100% above 600 K. Its rate constant predicted in the same temperature range (200−3000 K) can be given by

$$k_4 = 1.8 \times 10^{-34} T^{7.27} \exp[-8688/T] \text{ cm}^3/\text{s}$$

It is noteworthy that because the third term of the three-parameter rate expression is directly related to the reaction energies, one can estimate the uncertainties of the predicted rate constants, which are estimated to be the same as the uncertainties of the reaction energies discussed above.

Conclusions

From above presented discussion one can draw the following conclusions:

1. Reactions of W/W^+ with the water molecule are essentially multistate processes, during which lower-lying electronic states of the systems cross several times. They start with the formation of initial prereaction M(H_2O) complexes with M−H_2O bonding energies of 9.6 and 48.2 kcal/mol for M = W and W^+, respectively.

2. At the next stage, the insertion of metal center into O−H bond occurs with 20.0 and 53.3 kcal/mol barriers for neutral and cationic systems, respectively, and leads to the formation of HM(OH) products. The formed hydrido−metal−hydroxy complexes are 38.8 and 0.6 kcal/mol lower in energy than corresponding aqua complexes M(H_2O) for M = W and W^+, respectively. The overall process of M + H_2O → t-HM(OH) is calculated to be highly exothermic, 48.4 and 48.8 kcal/mol for M = W and W^+.

3. From the HM(OH) intermediate the reaction may proceed via several different channels, among which the stepwise HM(OH) → HMO + H → $(H)_2$MO and concerted HM(OH) → $(H)_2$MO pathways are more favorable and can compete (energetically) with each other. For the neutral system (M = W), the concerted process that occurs with 28.9 kcal/mol barrier is the most favorable one (calculated barrier on the stepwise pathway is 43.2 kcal/mol). In contrast, for the charged system (M = W^+), the stepwise pathway is slightly more favorable: the calculated barriers are 46.7 and 52.3 kcal/mol for stepwise

and concerted pathways, respectively. The ground-state to ground-state process *t*-HM(OH) → $(H)_2$MO is calculated to be exothermic by 30.5 and 15.3 kcal/mol for neutral and positively charged systems, and $(H)_2$MO species are global minima on the [MH_2O] PESs.

4. From the $(H)_2$MO intermediates the reactions proceed via H_2-molecule formation, which proceeds with a 53.1 kcal/mol activation barrier for the neutral system. For the singly charged system, H−H formation and dissociation is an almost barrierless process. The calculated ground-state to ground-state endothermicity of the (H_2)MO → H_2 + MO process is 30.7 and 24.3 kcal/mol for M = W and W^+, respectively.

5. The entire reaction of W and W^+ with the water molecule leading to H_2 + MO formation is found to be exothermic by 48.2 and 39.8 kcal/mol, respectively. In the gas phase with the collisionnless conditions the reactions $W(^7S) + H_2O \rightarrow H_2 + WO(^3\Sigma^+)$ and $W^+(^6D) + H_2O \rightarrow H_2 + WO^+(^4\Sigma^+)$ expected to proceed via a 10.4 and 5.1 kcal/mol overall energy barrier corresponding to the first O−H dissociation at the TS1.

Acknowledgment. We gratefully acknowledge (1) financial support from the Office of Naval Research under a MURI grant (Prime Award # N00014-04-1-0683 and Subaward # 2794-EU-ONR-0683) and (2) the Emerson Center for the use of its resources. S.X. thanks the Cherry L. Emerson Center of Emory University for a Visiting Fellowship.

Supporting Information Available: Complete ref 8; Table S1 of the B3LYP calculated relative energies (in kcal/mol, relative to the ground-state reactants) of the intermediates, transition states and products of the reactions W + H_2O and W^+ + H_2O for several low-lying electronic states; Table S2 of the B3LYP calculated total energies (in au) of the reactants, intermediates, transition states and products of the reactions W + H_2O and W^+ + H_2O for several low-lying electronic states; Table S3 of the calculated CCSD(T) energetics (in au) of the intermediates, transition states and products of the reaction of W and W^+ with water molecule at their B3LYP optimized geometries; Table S4 of Cartesian coordinates (in Å) of all reported structures. This material is available free of charge via the Internet at http://pubs.acs.org.

References and Notes

(1) (a) In *Structure/Reactivity and Thermochemistry of Ions*; Ausloos, P., Lias, S. G., Eds.; Reidel: Dordrecht, The Netherlands, 1987. (b) In *Gas*-Phase Inorg, Chemistry; Russell, D. H., Ed.; Plenum: New York, 1989. (c) *Selective Hydrocarbon Activation: Principles and Progress*; Davies, J. A., Watson, P. L., Liebman, J. F., Greenberg, A., Eds.; VCH: New York, 1990. (d) Eller, K.; Schwarz, H. *Chem. Rev.* **1991**, *91*, 1121. (e) In *Gas-Phase Metal Reactions*; Fontijn, A., Ed.; Elsevier: Amsterdam, 1992. (f) Weisshaar, J. C. In *Advances in Chemal Physics*; Ng, C., Ed.; Wiley-Interscince: New York, 1992; Vol. 81. (g) In *Transition Metal Hydrides*; Dedieu, A., Ed.; VCH: New York, 1992. (h) In *Bonding Energetics in Organometallic Compounds*; Marks, T. J., Ed.; ACS Symposium Series 428; American Chemical Society; Washington, DC, 1990; p 55. (i) Armentrout, P. B. In *Gas*-Phase Inorg. Chemistry; Russell, D. H., Ed.; Plenum: New York, 1989. (j) Armentrout, P. B.; Beauchamp, J. L. *Acc. Chem. Res.* **1989**, *22*, 315. (k) Armentrout, P. B. *Science* **1991**, *251*, 175. (l) Roth, L. M.; Freiser, B. S. *Mass Spectrom. Rev.* **1991**, *10*, 303. (m) Weisshaar, J. C. *Acc. Chem. Res.* **1993**, *26*, 213. (n) Irikura, K. K.; Beauchamp, J. L. *J. Am. Chem. Soc.* **1989**, *111*, 75. (o) Irikura, K. K.; Beauchamp, J. L. *J. Phys. Chem.* **1991**, *95*, 8344. (p) Schroder, D.; Schwarz, H. *Angew. Chem., Int. Ed. Engl.* **1995**, *34*, 1973, and references therein. (q) Haynes, C. L.; Chen, Y. M.; Armentrout, P. B. *J. Phys. Chem.* **1995**, *99*, 9110. (r) Chen, Y. M.; Armentrout, P. B. *J. Phys. Chem.* **1995**, *99*, 10775. (s) Bushnell, J. E.; Kemper, P. R.; Maitre, P.; Bowers, M. T. *J. Am. Chem. Soc.* **1994**, *116*, 9710. (t) van Koppen, P. A. M.; Kemper, P. R.; Bushnell, J. E.; Bowers, M. T. *J. Am. Chem. Soc.* **1995**, *117*, 2098. (u) Guo, B. C.; Castleman, A. W., Jr. *J. Am. Chem. Soc.* **1992**, *114*, 6152. (v) Guo, B. C.; Kerns, K. P.; Castleman, A. W., Jr. *J. Phys. Chem.* **1992**, *96*, 4879.

(2) Song, G.-M.; Wang, Y.-J.; Zhou, Y. *Int. J. Ref. Met. Hard* Mater. **2003**, *21*, 1.

(3) (a) Sasaki, N.; Hamamura, T. *Bull. Chem. Soc. Jpn.* **1956**, *29*, 365. (b) Hamamura, T. *Bull. Chem. Soc. Jpn.* **1959**, *32*, 1180. (c) Hamamura, T. *Bull. Chem. Soc. Jpn.* **1959**, *32*, 845. (d) Hamamura, T. *Bull. Chem. Soc. Jpn.* **1959**, *32*, 848. (e) Hamamura, T. *Bull. Chem. Soc. Jpn.* **1960**, *33*, 584.

(4) (a) Hamamura, T. *Sci.* Technol. **1960**, *9*, 1. (b) Hamamura, T. *Sci.* Technol. **1960**, *9*, 11. (c) Hamamura, T. *Sci.* Technol. **1960**, *9*, 13. (d) Hamamura, T. *Sci.* Technol. **1960**, *9*, 20.

(5) (a) Tamura, T.; Hamamura, T. *Bull. Chem. Soc. Jpn.* **1976**, *49*, 1780. (b) Tamura, T.; Hamamura, T. *Shinku* **1980**, *23*, 425. (c) Hamamura, T.; Tamura, T. *Shinku* **1982**, *25*, 98. (d) Hamamura, T.; Tamura, T.; Nakazawa, Y.; Inoue, K. *Shinku* **1985**, *28*, 289.

(6) (a) Ustinov, Y. K.; Ionov, N. I. *Zh. Tekh. Fiz.* **1967**, *37*, 2046. (b) Ageev, V. N.; Ionov, N. I.; Ustinov, Y. K. *Zh. Tekh. Fiz.* **1969**, *39*, 1337. (c) Goryachkovskii, Y. G.; Kostikov, V. I.; Solodkin, G. A. *Zh. Fiz. Khim.* **1976**, *50*, 1959.

(7) (a) Musaev, D. G.; Koga, N.; Morokuma, K. *J. Phys. Chem.* **1993**, *97*, 4064. (b) Musaev, D. G.; Morokuma, K. *Isr. J. Chem.* **1993**, *33*, 307. (c) Musaev, D. G.; Morokuma, K.; Koga, N.; Nguyen, K. A.; Gordon, M. S.; Cundari T. R. *J. Phys. Chem.* **1993**, *97*, 11435. (d) Musaev, D. G.; Morokuma, K. *J. Chem. Phys.* **1994**, *101*, 10697. (e) Musaev, D. G.; Morokuma, K. *J. Phys. Chem.* **1996**, *100*, 11600. (f) Perry, J. K.; Ohanessian, G.; Goddard, W. A., III. *J. Phys. Chem.* **1993**, *97*, 5238. (g) Perry, J. K.; Ohanessian, G.; Goddard, W. A., III. *Organometallics* **1994**, *13*, 1870. (h) Blomberg, M. R. A.; Siegbahn, P. E. M.; Svensson, M. *J. Phys. Chem.* **1994**, *98*, 2062. (i) Siegbahn, P. E. M.; Blomberg, M. R. A.; Svensson, M. *J. Am. Chem. Soc.* **1993**, *115*, 4191. (j) Michelini, M. C.; Russo, N.; Sicilia, E. *Inorg. Chem.* **2004**, *43*, 4944. (k) Chiodo, S.; Kondakova, O.; Michelini, M. C.; Russo, N.; Sicilia, E.; Irigoras, A.; Ugalde, J. M. *J. Phys. Chem. A* **2004**, *108*, 1069. (l) Michelini, M. C.; Sicilia, E.; Russo, N.; Alikhani, M. E.; Silvi, B. *J. Phys. Chem. A* **2003**, *107*, 4862. (m) Michelini, M. C.; Russo, N.; Sicilia, E. *J. Phys. Chem. A* **2002**, *106*, 8937. (n) Sicilia, E.; Russo, N. *J. Am. Chem. Soc.* **2002**, *124*, 1471.

(8) Frisch, M. J.; et al. *Gaussian 03*, revision C1; Gaussian, Inc.: Pittsburgh, PA, 2003.

(9) (a) Becke, A. D. *Phys.* Rev. A **1988**, *38*, 3098. (b) Lee, C.; Yang, W.; Parr, R. G. *Phys.* Rev. B **1988**, *37*, 785. (c) Becke, A. D. *J.* Chem. Phys. **1993**, *98*, 5648.

(10) Moreria, I. de P. R.; Illas, F.; Martin, R. L. *Phys. Rev. B* **2002**, *65*, 155102, and references therein.

(11) (a) Bauschlicher, C. W., Jr.; Ricca, A. *J. Phys. Chem.* **1994**, *98*, 12899. (b) Russo, T. V.; Martin, R. L.; Hay, P. J. *J. Chem. Phys.* **1995**, *102*, 8023. (c) Rodriguez-Santiago, L.; Sodupe, M.; Branchadell, V. *J. Chem. Phys.* **1996**, *105*, 9966. (d) Siegbahn, P. E. M.; Crabtree, R. H. *J. Am. Chem. Soc.* **1997**, *119*, 3103.

(12) (a) Schwerdtfeger, P.; Dolg M.; Schwarz, W. H.; Bowmaker, G. A.; Boyd, P. D. W. *J.* Chem. Phys. **1989**, *91*, 1762. (b) Andrae, D.; Haubermann, U.; Dolg, M.; Stoll, H.; Preuss, H. *Theor.* Chim. Acta **1990**, *77*, 123. (c) Bergner, A.; Dolg M.; KŸchle, W.; Stoll, H.; Preuss, H. *Mol.* Phys. **1993**, *80*, 1431.

(13) Fukui, K. *Acc. Chem. Res.* **1981**, *14*, 363

(14) Klippenstein, S. J.; Wagner, A. F.; Dunbar, R. C.; Wardlaw, D. M.; Robertson, S. H. *Variflex* **1999**.

(15) Chase, M. W., Jr. *NIST-JANAF Thermchemical Tables*, 4th ed.; J. Phys. Chem. Ref. Data, Monograph 9; Woodbury, New York, 1998, 1.

(16) Campbell-Miller, M. D.; Simard, B. *J. Opt. Soc. Am. B* **1996**, *13*, 2115.

(17) Blagojevic, V.; Koyanagi, G. K.; Lavrov, V. V.; Orlova, G.; Bohme, D. K. *Chem. Phys. Lett.* **2004**, *389*, 303.

(18) Zhang, X.-G.; Rue, C.; Shin, S.-Y.; Armentrout, P. B. *J. Chem. Phys.* **2002**, *116*, 5574.

(19) Lu, C.-W.; Chou, S.-L.; Lee, Y.-P.; Xu, S. C.; Xu, Z. F.; Lin, M. C. *J. Chem. Phys.* **2005**, *122*, 244314.

(20) Moore, C. E. *Atomic Energy Levels, NSRD-NBS., USA*; U.S. Goverment Printing Office: Washington, DC, 1991; Vol. 1.

(21) Martin, R. L.; Hay, P. J. *J. Chem. Phys.* **1981**, *75*, 4535.

(22) (a) Zhu, R. S.; Lin, M. C. *J. Phys. Chem. A* **2001**, *105*, 6243. (b) Zhu, R. S.; Xu, Z.-F.; Lin, M. C. *J. Chem. Phys.* **2004**, *120*, 6566. (c) Xu, S. C.; Zhu, R. S.; Lin, M. C. *Int. J. Chem. Kinet.*, in press.